The first case of microsporidiosis in *Paramecium*

Yulia Yakovleva[a], Elena Nassonova[b, c], Natalia Lebedeva[d], Olivia Lanzoni[e], Giulio Petroni[e], Alexey Potekhin[f], Elena Sabaneyeva[a,*]

[a] Department of Cytology and Histology, Saint Petersburg State University, Universitetskaya emb. 7/9, 199034 Saint Petersburg, Russian Federation, st041958@student.spbu.ru (YY), e.sabaneeva@spbu.ru (ES)

[b] Laboratory of Cytology of Unicellular Organisms, Institute of Cytology RAS, Tikhoretsky ave. 4, 194064 Saint Petersburg, Russian Federation, nosema@mail.ru

[c] Department of Invertebrate Zoology, Saint Petersburg State University, Universitetskaya emb. 7/9, 199034 Saint Petersburg, Russian Federation, e.nassonova@spbu.ru

[d] Core Facility Center for Cultivation of Microorganisms, Saint Petersburg State University, Peterhof, Botanicheskaya st. 17, 198504 Saint Petersburg, Russian Federation, nalebedeva@yandex.ru

[e] Department of Biology, University of Pisa, via A Volta 4, 56126, Pisa, Italy, oli.lanzoni@gmail.com (OL), giulio.petroni@unipi.it (GP)

[f] Department of Microbiology, Saint Petersburg State University, 16th line, Vasilyevsky Island, 29, 199178 Saint Petersburg, Russian Federation, alexey.potekhin@spbu.ru

Running title: Microsporidiosis in *Paramecium*

***Corresponding author:** Elena Sabaneyeva, Department of Cytology and Histology, Saint Petersburg University, Universitetskaya emb. 7/9, 199034 Saint Petersburg, Russian Federation, tel.: +78123289687, e-mail: e.sabaneeva@spbu.ru

This is an Accepted Manuscript for Parasitology. This version may be subject to change during the production process. DOI: 10.1017/S0031182020000633

Abstract

A new microsporidian species, *Globosporidium paramecii* gen. nov., sp. nov., from *Paramecium primaurelia* is described on the basis of morphology, fine structure, and SSU rRNA gene sequence. This is the first case of microsporidiosis in *Paramecium* reported so far. All observed stages of the life cycle are monokaryotic. The parasites develop in the cytoplasm, at least some part of the population in endoplasmic reticulum and its derivates. Meronts divide by binary fission. Sporogonial plasmodium divides by rosette-like budding. Early sporoblasts demonstrate a well-developed exospore forming blister-like structures. Spores with distinctive spherical shape are dimorphic in size (3.7 ± 0.2 and 1.9 ± 0.2μm). Both types of spores are characterized by a thin endospore, a short isofilar polar tube making one incomplete coil, a bipartite polaroplast, and a large posterior vacuole. Experimental infection was successful for 5 of 10 tested strains of the *Paramecium aurelia* species complex. All susceptible strains belong to closely related *P. primaurelia* and *P. pentaurelia* species. Phylogenetic analysis placed the new species in the Clade 4 of Microsporidia and revealed its close relationship to *Euplotespora binucleata* (a microsporidium from the ciliate *Euplotes woodruffi*), to *Helmichia lacustris* and *Mrazekia macrocyclopis*, microsporidia from aquatic invertebrates.

Key words: intracellular parasitism, host specificity, microsporidia, phylogeny, *Globosporidium*, ciliate, *Paramecium*

Introduction

Microsporidia is a group of obligate intracellular parasitic protists, relative to rozellids, aphelids and fungi (Karpov *et al.*, 2014; Keeling, 2014; Bass *et al.*, 2018). Microsporidian infections are common in many groups of Metazoa, mostly in insects and crustaceans among invertebrates (Stentiford and Dunn, 2014), and in fish among vertebrates (Lom and Nielsen, 2003). Microsporidia infect commercially important animals, sometimes occur in immunocompromised humans, and are considered to be opportunistic pathogens (Didier and Weiss, 2006; Stentiford *et al.*, 2016). Surprisingly, though the host range of microsporidia is very wide, they have been rarely reported in protists. Among these, a moderate number of infections with microsporidia and closely related organisms has been registered mostly in gregarines (Sokolova *et al.*, 2013, 2014; Larsson, 2014) and amoebae (Michel *et al.*, 2000, 2009a,b, 2012). Taking into account basal position and primitive organization of metchnikovellids infecting gregarines (Mikhailov *et al.*, 2017; Galindo *et al.*, 2018) and rozellids infecting amoebae (Corsaro *et al.*, 2014a,b, 2016; Quandt *et al.*, 2017), one could expect microsporidian species infecting other protists fall into the most primitive clades as well. However, according to Fokin *et al.* (2008) and Stentiford *et al.* (2017), and as we show here, this assumption seems to be misleading, at least, in what concerns the species invading ciliates and paramyxids.

Ciliates are often infected by prokaryotic or eukaryotic microorganisms (Kodama and Fujishima, 2009; Görtz, 2010; Nowack and Melkonian, 2010; Fokin, 2012; Castelli *et al.*, 2019; Fokin, 2019), however, only a few cases of microsporidian infection have been registered in ciliates so far (Foissner and Foissner 1995; Fokin *et al.*, 2008), most of the records being fragmentary and species descriptions incomplete. Only light microscopic observations have been made of *Nosema balantidii* in *Balantidium* sp. (Lutz and Splendor, 1908), *Gurleya nova* in *Spirobutschliella chattoni* (Hovasse, 1950), and *Glugea campanellae* in *Campanella umbellaria* (Krüger, 1956). Fine structure of microsporidia from *Stentor roeseli* and *Stentor polymorphus* (Görtz, 1987) and of *Ciliatosporidium platyophryae* from *Platyophrya terricola* (Foissner and Foissner, 1995) has been studied by means of transmission electron microscopy (TEM). Three other microsporidia have been observed in *Frontonia leucas*, *Sonderia vorax* and *Vorticella* sp. (Fokin *et al.*, 2008); however, none of them has been studied in detail. Actually, by now the only microsporidium parasitizing ciliates, which has received full morphological and molecular characterization, is *Euplotespora binucleata* inhabiting the cytoplasm of *Euplotes woodruffi* (Fokin *et al.*, 2008). According to the phylogenetic reconstructions based on small subunit (SSU) rRNA gene analysis, *E. binucleata* clusters with microsporidian genera *Cystosporogenes* and *Vittaforma* (Fokin *et al.*, 2008), which are by no means primitive. Such cases provoke great interest, as studying microsporidian infections in protists could shed light on the host-parasite

interactions at the cellular level as well as on evolutionary pathways of these enigmatic intracellular parasites, which, apparently, comprise both, reductive evolution and metabolic specialization (Keeling *et al.*, 2014).

A spherical eukaryotic microorganism was revealed in the cytoplasm of a strain of ciliates belonging to *P. aurelia* complex isolated from the environmental sample collected in Malaga, Spain. Based on its morphological features and SSU rDNA sequence, the endobiont was identified as a novel microsporidian species. Referring to the specific regular spherical shape of its spore, we propose the name *Globosporidium paramecii*, gen. nov., sp. nov.

Materials and Methods

Cell cultures

Paramecium aurelia strain SpM5-3 harboring a spherical microorganism in the cytoplasm was isolated from a pool in Guadalmedina riverbed in Malaga, Spain (36°44'53.6"N, 4°25'28.8"W) in 2015. The list of endobiont free strains used in experimental infections as recipient cells is given in Table 1. Almost all cultures were maintained and kindly provided by Core Facility Center "Cultivation of microorganisms" (RC CCM). The cultures were maintained in the lettuce infusion inoculated with *Klebsiella aerogenes* at room temperature. The original strain was cultivated in several replicates kept under different temperatures (24°C and 16°C) and various feeding intensity.

Living cell observations and experimental infections

Living host cells were immobilized and squashed with a compression device (Skovorodkin, 1990) and analyzed using differential interference contrast (DIC) with a Leica 6000 microscope (Leica Microsystems, GmbH, Wetzlar, Germany) equipped with a digital camera DFC 500.

In most experimental infections, we used a blind study design: the species identity of the recipient strains of the *P. aurelia* complex was established only after the end of the experiment, with the exception of *P. pentaurelia* 87, Nr1-9 and *P. caudatum* strains. For experimental infection, 0.5 ml of the culture medium taken from the bottom of the tubes containing infected paramecia of the SpM5-3 strain was put in a well and checked for the presence of ciliates under a dissecting microscope. If present, all paramecia of the original culture were removed and replaced with 25-30 cells of a recipient strain. The ciliates were checked for the infection on the 3rd, 7th and 14th day after the beginning of the experiment using DIC. For each recipient strain, the experiment was repeated 3 times. In another set of experimental infections, the cells of the

susceptible strains were infected as described above and checked on the 1st day both by DIC and by means of DAPI staining. In case *P. caudatum* strain was used as the recipient, the cells of the infected *P. aurelia* strain were not removed from the recipient cells, as *P. caudatum* are easily distinguished from species of the *P. aurelia* complex by the morphology of the micronucleus.

Spore measurements were performed using DIC images of living microsporidia. Standard deviation was calculated using STATISTICA 10 software.

Permanent staining procedures

To prepare thin sections, *Paramecium* cells were fixed with Bouin's fluid, thoroughly washed in 70° ethanol, rinsed in distilled water and mounted in 3% low melting agarose. Small agarose blocks with ciliates were cut out, dehydrated in a series of alcohol and embedded in paraffin. Paraffin blocks were sectioned to obtain 6 µm thick sections. The sections were stained with hematoxylin and eosin.

For squashed cell preparation, 2-3 paramecia were placed on a slide in a small drop of culture medium. Cells were crushed with a needle and immediately fixed either with ice-cold 100% methanol or with Bouin's fluid. Methanol-fixed slides were further stained by Giemsa (Sigma, USA) according to the manufacturer protocol or subjected to periodic acid-Schiff (PAS) staining procedure (Vávra, 1959). For PAS staining, the slides were rinsed in distilled water, treated with 0.5-1% periodic acid for 5 min, thoroughly washed for 10 min and stained with Schiff's reagent for 30 min. Then the slides were washed with the sulphurous acid solution, rinsed in distilled water, dehydrated and mounted in Canada balsam. Bouin-fixed slides were proceeded as follows: the fixative was removed and exchanged for 70% alcohol, then the slides were rinsed in distilled water, subjected to hydrolysis in 6N HCl for 25 min, washed in distilled water and stained with 1% basic fuchsin solution for 30 min. After rinsing in distilled water and ~~a~~ brief immersion in acidic 70% alcohol, the slides were counterstained with light green, dehydrated in a series of alcohol and mounted in Canada balsam or Damarlack.

Semi-thin sections of paramecia were obtained using the material embedded for TEM and the same equipment (see Transmission Electron Microscopy). 700 nm thick sections were stained with 1% methylene-blue at 70°C for 20 sec, washed in distilled water and stained with 1% basic fuchsin at 70°C for 20 sec. Slides were examined using the same microscope as used for living cell observations.

For DAPI staining, ciliates were transferred onto adhesive slides (SuperFrost, Menzel, Germany), fixed with 4% paraformaldehyde (PFA) in PBS (7.2-7.4), washed with PBS and postfixed with 70% methanol. The slides were mounted in Mowiol (Mowiol 4.88, Calbiochem) diluted in glycerol containing p-phenylenediamine and DAPI (4',6-diamidino-2-phenylindole)

according to the manufacturer protocol. The slides were analyzed with a Leica TCS SPE2 Confocal Laser Scanning Microscope. The images were further processed with Fiji open-access software (Schindelin *et al.*, 2012).

Transmission Electron Microscopy

Paramecium cells were fixed and proceeded as described in Szokoli *et al.*, (2016). The cells were fixed in a mixture of 1.6% PFA and 2.5% glutaraldehyde in 0.1 M phosphate buffer (pH 7.2-7.4) for 1.5 h at room temperature, washed in the same buffer containing sucrose (12.5 %) and postfixed in 1.6% OsO_4 for 1 h at 4°C. After dehydration in an ethanol gradient followed by ethanol/acetone (1:1) and 100% acetone, the cells were embedded in Epoxy embedding medium (FlukaChemie AG, BioChemika, St. Gallen, Switzerland) according to the manufacturer protocol. The blocks were sectioned with a Leica EM UC6 Ultracut. Ultrathin sections were stained with aqueous 1% uranyl acetate followed by 1% lead citrate. All samples were examined with a JEOL JEM-1400 (JEOL, Ltd., Tokyo, Japan) electron microscope at 80 kV. The images were obtained with an inbuilt digital camera.

DNA isolation, PCR amplification and sequencing

For total DNA extraction of the strain SpM5-3, approximately 80 *Paramecium* cells were fixed in 70% ethanol. DNA was extracted following the CTAB protocol or using NucleoSpin® Plant DNA Extraction Kit (Macherey-Nagel GmbH & Co. KG, Düren NRW, Germany), for fungal mycelium. The microsporidian SSU rDNA was amplified by PCR using forward primer V1f and reverse primer 1492r (Zhu *et al.*, 1993; Weiss and Vossbrinck, 1999).

Thermal cycle parameters were: initial denaturation (10 min at 95 °C) followed by 39 cycles of 30 s at 94 °C, 60 s at 50 °C and 120 s at 72 °C, followed by 10 min at 72 °C for the final extension. The size of the amlicon for microsporidian SSU rRNA gene was approximately 1500 bp. Amplicons were purified using Cleanup mini Purification Kit (Eurogene). The sequencing reactions were carried out with the aforementioned primers and with the internal primer 530r (Weiss and Vossbrinck, 1999) using BigDye® Terminator v3.1 Cycle Sequencing Kit (Applied Biosystems™) and analyzed with Applied Biosystems® 3500xL Genetic Analyzer.

The final length of the assembled contig after the removal of flanking regions for the primers was 1135 bp.

Alignment and phylogenetic inferences

The alignment including the available sequences of described species of Microsporidia from Clade 4 and 10 sequences of species from Clade 5 (Vossbrinck *et al.*, 2014) was created

using MUSCLE algorithm (Edgar, 2004) implemented in SeaView v. 4.3.5 (Gouy *et al.*, 2010) with the following manual editing. The final dataset for SSU rRNA analysis included 55 taxa and 1295 positions. The maximum likelihood (ML) phylogenetic analysis was performed using RAxML 8.1.24 program (Stamatakis, 2014) at CIPRES portal (Miller *et al.*, 2010). GTR+γ model of evolution with 25 substitution rate categories was applied. 100 independent ML inferences with distinct randomized MP starting trees were performed; the best-scoring tree was tested using non-parametric bootstrapping (1000 pseudoreplicates). Bayesian analysis was performed with MrBayes 3.2.1 (Ronquist *et al.*, 2012) using GTR model with gamma correction for intersite rate variation (8 categories) and the covarion model. Trees were run as two separate chains (default heating parameters) for 10 million generations, by which time they had ceased converging (final average standard deviation of the split frequencies was less than 0.01), the first 25 % of generations were discarded for burn-in.

Paramecium COI gene sequencing

As cryptic species of the *P. aurelia* complex cannot be distinguished on the basis of the SSU rRNA gene sequencing, identification of the host species and of the strains used in the experimental infections was performed by COI gene sequencing (Strüder-Kypke and Lynn, 2010). For COI gene sequencing of the original host strain SpM5-3, DNA was amplified and directly sequenced as described elsewhere (Lanzoni *et al.*, 2016, 2019).

Results

Host species identification and experimental infection

Paramecium strain SpM5-3 harbouring *G. paramecii* in the cytoplasm was isolated from a population collected in a pool in Guadalmedina riverbed in Malaga, Spain, in 2015 (Fig. 1 A-C). Based on the ciliate morphological characters, primarily the number and the type of micronuclei, the host strain was attributed to *P. aurelia* complex of species (Fokin, 2010). Molecular characterization using the sequencing of the host cytochrome c oxidase subunit I (COI) gene placed the host within *P. primaurelia* (100% sequence identity, GenBank Accession number: MG589322). As estimated by the analysis of 150 DAPI stained paramecia, this environmental *Paramecium* strain showed 100% prevalence of microsporidian infection.

The results of experimental infection with *G. paramecii* are shown in Table 1. The experiments were designed as a blind study: the species identity of most of the recipient strains was established by COI gene sequencing only after the results of the experimental infections had been obtained. Among the 10 strains belonging to *P. aurelia* complex of species, used as recipients in the experimental infections, only 5 (IP3-20, NR-2, CyL8-8, 87 and Nr1-9) proved to

be susceptible to the infection with *G. paramecii* (Fig. 1 D-M). This result was consistent for each strain in all 3 repeats of the experiment. Two of these strains (IP3-20 and CyL8-8) were identified as *P. primaurelia*, like the host strain SpM5-3, and the three other susceptible strains (NR-2, 87 and Nr1-9) belonged to *P. pentaurelia*. The resistant strains belonged to *P. biaurelia* (IP1-2 and ETu7-11), *P. triaurelia* (Sp9-33), *P. novaurelia* (UB-15) and *P. sonneborni* (CyL10-4). *P. pentaurelia* strains demonstrated differences in the course of infection: the strain 87/5 quickly acquired infection, but tended to die out during the second week of the experiment (in all 3 repeats), while it took much longer to develop the infection in the strains NR-2 and Nr1-9. However, in the two latter strains, the infection appeared to be stable, and the host cells did not die by the end of the experiment. The cells of BMK15-1 population of *P. caudatum* were never infected. On the contrary, VL18-5 strain of *P. caudatum*, susceptible to infection with various bacterial endosymbionts belonging to *Holospora* genus, got infected on the first day, but died out by the third day after the beginning of the experiment as a result of hyperinfection.

In all experiments, in the susceptible *P. primaurelia* strains and in NR-2 *P. pentaurelia* strain the infection rate was 100% on the third day after the beginning of the experiment and did not change in the course of time. The first spores were registered both with DIC and 4′,6-diamidino-2-phenylindole (DAPI) staining in the susceptible cells as early as 24 h after the beginning of the experiment (Supplementary material Fig. 1 B). In 3 days the number of spores increased, and the experimentally infected cells did not differ from the cells of naturally infected paramecia. For the *Paramecium primaurelia* strain IP3-20 the infection was stable for more than half a year, while for *P. pentaurelia* NR-2 - for more than a year. In one experiment, the *P. primaurelia* strain CyL8-8 died out by the 7th day after the beginning of the experiment, in two other experiments the infection was stable in this strain for about 3 months, then the strain became extinct.

In some replicates, the parasites were spontaneously lost, apparently, due to host cell starvation.

Morphology of the life stages of the parasite as revealed by light microscopy

Infected paramecia of the isolated SpM5-3 strain and cells obtained in the course of experimental infections had a normal appearance and did not manifest any signs of movement or physiological disorders. Light microscopy analysis using DIC revealed in the cytoplasm of immobilized and squashed SpM5-3 paramecia of the strain very uniform, regular, spherical non-refractive spores, most often showing a depression-like structure at one side, which we considered a posterior vacuole (Fig. 1 A, B). As a rule, the spores occurred singly and did not form groups. The parasites were distributed evenly in the host cytoplasm, showing no preference

to any particular region of the cell. The number of spores per host cell varied depending on the nutritional state of the culture from about half a dozen in starved cells to several dozen in well-fed cultures. Some of the spores were observed in direct contact with the host cytoplasm, while others were enclosed in an individual vesicle (Fig. 1 B, L). Here and hereinafter, the term "vesicle" stands for a vacuole with the envelope of unknown origin. As measured in DIC images, the diameter of the spores in living and squashed host cells of the isolated from nature strain SpM5-3 ranged from 3.3 to 4.2 µm, average 3.7±0.2µm (n=41; here and hereinafter, mean±SD), and these spores were considered large. Alongside with the large spores, in experimentally infected *Paramecium* cells, an additional population of spores, which were designated "small" due to their diameter ranging from 1.6 to 2.2 µm, av. 1.9±0.2µm (n=20), was frequently found (Fig. 1 E). Besides the spores, the host cytoplasm abounded in numerous proliferative stages of the life cycle, easily distinguishable from the spores by their lower optical density, which made them nearly transparent in DIC. These stages could be better discerned in squashed ciliates (Fig. 1 C, F-J). Proliferative stages differed in their morphology, with mononuclear, dividing binuclear, and tetranuclear cells found among them (Fig. 1 D, F-H). All binuclear cells were considered dividing, as we never observed typical diplokarya with two nuclei tightly apposed. In DIC images, the early proliferative stages, mononuclear or dividing binuclear meronts, seemed to be in direct contact with the host cytoplasm, while later stages, binuclear and tetranuclear sporonts, were always found enclosed in vesicles (Fig.1 F-J), which became especially visible in the squashed host cells, when the rupture of the host pellicle led to osmotic shock and caused swelling of host vesicles and mitochondria, as well as of proliferative stages and sporoblasts (Fig. 1 C, F, G, I, J). Swelling of these stages made estimation of their actual size using DIC images impossible. Noteworthy, optically dense spores with pronounced posterior vacuole were never swollen, apparently, due to a well-developed cell wall.

Sporonts and sporoblasts were arranged in groups of 2, 4, or 6 within a vesicle (Fig. 1 C, F, I, J). Interestingly, in experimentally infected cells, the large spores were occasionally observed enclosed in the host cell vesicles surrounding guanine/hypoxanthine crystals (Fig. 1 M), while sporoblasts sometimes resided in the perinuclear space of the host macronucleus (Fig. 1 K). Occasionally, in experimentally infected *P. caudatum*, we managed to observe the large spores with the ejected polar tube inside the host food vacuole (Fig. 1 N). The length of the stretched polar tube was about 3 times longer than the spore and reached 9-10.5 µm.

Permanently stained slides were prepared using both, originally infected *P. primaurelia* strain SpM5-3 and experimentally infected *P. primaurelia* strain IP3-20 and *P. pentaurelia* strain NR-2 (Fig. 2). Although the standard hematoxylin-eosin staining of paraffin sections did not permit to clearly distinguish the proliferative stages of microsporidia in paramecia, as the

staining pattern in ciliates differed significantly from the one seen in Metazoa with the same technique, the spores could still be discerned (Fig. 2 A). In semi-thin sections of the originally infected paramecia embedded in epoxy resin and stained with methylene blue and fuchsin, alongside with the spores, proliferative stages were easily visualized, albeit less intensively stained (Fig. 2 B-D). Among these, dividing binucleate stages and three-lobed plasmodia occurred very often, suggesting constant autoinvasion of the host. Similar to living cell observations, some spores were seen inside the individual vesicles (Fig. 2 B), while most of the spores resided directly in the host cytoplasm, without any visible surrounding membrane. Contrary to DIC images, in semi-thin sections, we have never observed any vesicles surrounding sporonts and sporoblasts. In some spores a transparent colorless posterior vacuole could be clearly discerned, which could be distinguished from the fuchsin stained nucleus (Fig. 2 B). The spores and the proliferative stages were also apparent in the squashed host cells stained with Giemsa (Fig. 2 E), however, the nuclei of all stages were much more distinct in the squashed host cells stained with fuchsin and counterstained with light green (Fig. 2 F-I). Besides mononuclear spores, binuclear dividing stages and tetranuclear plasmodia were revealed, which was in good concordance with our living cell observations and images of semi-thin sections. Likewise, in fixed cells, we never observed diplokarya with two apposed nuclei. Structures resembling small spores often occurred in the squashed host cell preparations; however, owing to the harsh treatment applied in the course of the procedure, we refrained from taking them into consideration, as they could be easily confused with the cell debris. A short polar tube and an anchoring disk were conspicuous in the spores released from the squashed host cells and processed using periodic acid-Schiff (PAS) reaction (Supplementary material Fig. 1 A), which is applied to reveal the components of the extrusion apparatus in microsporidia (Vávra, 1959).

In DAPI stained paramecia of both, naturally and experimentally infected strains, besides the host's macronucleus and two micronuclei, nuclei of numerous parasites were always revealed. In all examined host cells, two types of parasites' nuclei, differing in size and signal intensity, were present, bigger nuclei demonstrating weaker fluorescence (Supplementary material Fig. 1 B). This dissimilarity argues for different rate of nuclear chromatin condensation in the spores and proliferative life stages of the parasite. Merging bright field microscopy images with the corresponding images of DAPI fluorescence obtained with confocal microscopy made it possible to clearly distinguish the nucleus of *G. paramecii* from the posterior vacuole (Supplementary material Fig. 2 C) and confirm that the depression seen with DIC corresponds to the posterior vacuole.

Fine structure of the life cycle stages

Nearly all life cycle stages were observed in the cytoplasm of the original naturally infected *P. primaurelia* strain SpM5-3 examined with TEM (Fig. 3 A, B). The earliest observed stage, meronts, had an irregular shape, one nucleus (up to 1.5 μm in diameter) and dense homogeneous cytoplasm containing numerous free ribosomes (Fig. 3 C, D). Meronts divided by binary fission, as evidenced by the presence of binucleate cells, which have not undergone cytokinesis yet (Fig. 3 E, F). Sporonts, like meronts, were monokaryotic, but could be easily distinguished from the latter stage by the presence of electron-dense patches on their plasma membrane, presumably, the primordium of the exospore (Fig. 4 A). The cytoplasm of sporonts seemed less homogeneous than in meronts, and cisternae of the endoplasmic reticulum (ER) appeared. Sporogonial plasmodium divided by rosette-like budding, showing at least four monokaryotic lobes in one plane (Fig. 4 B). The sporogonial plasmodium, like early sporonts, demonstrated patches of electron-dense material on their surface. In early sporoblasts, the exospore was much more developed and interrupted just in a few sites (Fig. 4 C). Sometimes blister-like structures were formed. The shape of the early sporoblasts seemed less irregular than that of meronts and sporonts, probably, due to the developing cell wall. Numerous cisternae of the ER became clearly visible. Late sporoblasts could be characterized by the presence of a fully developed exospore and a more regular cell shape, which gradually became oval (Fig. 4 D, E, F). At this stage, a primordial polar tube (Fig. 4 D, E), an anchoring disk (Fig. 4 E), and a developing polaroplast could be registered (Fig. 4 F). In TEM sections, spores of two size classes were revealed (Fig. 5 A, B), supporting the observations of living cells made with DIC. Both types of spores had a specific regular spherical shape, were always mononuclear and were characterized by a well-pronounced pattern of ER cisternae, often forming stacks parallel to the plasma membrane. Large spores ranged from 2.0 to 3.0μm in diameter, av. 2.4±0.3 μm (n=23), while the small spores ranged from 0.9 to 1.4 μm in diameter, av. 1.2±0.1 μm (n=16) (Fig. 5). Neither type of spores ever formed groups. Mature spores possessed a two-layered cell wall (about 57-87 nm thick) comprising the electron lucid endospore (24-40 nm thick in the large spores, and 13-17 nm thick in the small ones), adjacent to the plasma membrane, and the electron-dense exospore (29-47 nm thick in the large spores, and 25-40 nm thick in the small ones) (Fig. 6 C, D). The outer layer of the latter sometimes peeled off forming protrusions into the host cytoplasm (Fig. 5 D, E). As seen in cross-sections made at various angles, in spores of both types (in maturating as well as in mature spores) two parts of polaroplast were observed (Fig. 5 C, D, Fig.6 C, D). The anterior part by small vesicles with similar contents, and the posterior part is represented by a large sac with homogeneous contents (Fig. 5 C, D, Fig. 6 C, D). A fully developed polar sac- anchoring disk complex had a typical mushroom-like structure and

was connected to a short isofilar polar tube (Fig. 5 C-F) making one incomplete coil (a semi-coil) (Fig. 5 F). A large posterior vacuole was observed in both types of the spores (Fig. 5 A, Fig. 6 A). Inside it, a vesicle containing some electron-dense material, most likely, the cross-sectioned polar tube, could occasionally be visualized (Fig. 6 A).

Phylogeny

In the phylogenetic reconstructions based on the analysis of SSU rRNA gene, *G. paramecii* was placed within Terresporidia in Clade IV *sensu* Vossbrinck and Debrunner-Vossbrinck (2005), which corresponds to Clade 4 *sensu* Vossbrinck *et al.* (2014) and Clade IV, subclade B *sensu* Williams *et al.* (2018) (Fig. 7). It clusters together with *Euplotespora binucleata*, the only sequenced microsporidia from ciliates, and with the species infecting mainly the intestinal epithelium of insect and crustacean hosts (with one remarkable exception – human microsporidia *Vittaforma corneae*). Based upon SSU rRNA gene sequence, *G. paramecii* is most closely related to *E. binucleata* (DQ675604, 88.3% sequence similarity), infecting the brackish water ciliate *Euplotes woodruffi*, to *Mrazekia macrocyclopsis* (FJ914315, 87.6% sequence similarity), a parasite of the copepod *Macrocyclops albidus*, and to *Helmichia lacustris* (GU130406, 79.2 % sequence similarity), a parasite of the larvae of the midge *Chironomus plumosus*.

Discussion

Globosporidium paramecii possesses several morphological features of its spore, which are considered typical of "higher" microsporidia: a polar sac-anchoring disk complex, a bipartite polaroplast, a posterior vacuole and a well-developed polar tube (Han and Weiss, 2017). In *G. paramecii*, the anterior part of polaroplast is vesicular, resembling the one observed in the microsporidium from *Stentor* (Görtz, 1987) and not lamellar, like in other microsporidia infecting ciliates, e.g. *E. binucleata* from *Euplotes woodruffi*, which also falls into the same clade (Fokin *et al.*, 2008) as *G. paramecii*, and the parasite of *Platyophria terricola*, *C. platyophryae*, whose phylogenetic position is still unknown (Foissner and Foissner, 1995). The endospore, though conspicuous, is very thin, like that of microsporidium from *Stentor* (Göertz, 1987) with unknown phylogenetic position, and *E. binucleata* (Fokin *et al.*, 2008). Interestingly, other representatives of Clade IV, closely related to *G. paramecii*, such as *Helmichia lacustris*, infecting Chironomidae (Tokarev *et al.*, 2012), *Mrazekia macrocyclopis*, a parasite of Copepoda (Issi *et al.*, 2010) and *Cystosporogenes* sp. from Coleoptera (Kyei-Poku *et al.*, 2011) possess thicker endospore (see Supplementary Table S1). One could hypothesize, that the thickness of the endospore, which is made of chitin and proteins (Vávra and Lukeš, 2013), might depend on

the host environment: in terrestrial hosts the endospore of microsporidia is thicker to protect the spore from dessication, while in aquatic hosts it is thin, as there is no risk of drying out. The thicker endospore of *C. platyophryae*, parasitizing the terrestrial ciliate *P. terricola* (Foissner and Foissner, 1995), corroborates this assumption.

G. paramecii has two types of spores, differing in size, but with similar shape and fine structure. Both types of spores of *G. paramecii* are characterized by the presence of a short isofilar polar tube, which makes one incomplete coil. Similar polar tubes have been described in two other microsporidian species from ciliates, i.e. in *E. binucleata* (Fokin *et al.*, 2008) and in *Ciliatosporidium platyophryae* (Foissner and Foissner, 1995). According to the images provided by Görtz, the polar tube of microsporidium infecting *Stentor* is short as well (Görtz, 1987). Those representatives of Clade 4, which group together with *G. paramecii*, either have a short uncoiled tube, like *Helmichia lacustris*, infecting *Chironomus plumosus* (Tokarev *et al.*, 2012) or have a rather short polar tube making 3-4 coils, as in *Mrazekia macrocyclopsis* (Issi *et al.*, 2010), while others possess longer polar tubes, making 10-11 coils, like *Cystosporogenes* sp. from the beetle *Agrilus anxius* (Kyei-Poku *et al.*, 2011). Though representatives of Clade IV, subclade B *sensu* Williams *et al.* (2018) demonstrate extensive variability of morphological features, all of them (with a remarkable exception, *Mrazekia macrocyclopsis*) possess a well-developed extrusion apparatus with a bipartite polaroplast and a rather short isofilar polar tube making up to 10-11 coils arranged in a single row (see Supplementary Table S1). The occurrence of a short uncoiled or slightly coiled filament in the representatives of this Clade has been proposed to be a result of reductive evolution (Tokarev *et al.*, 2012). These species rarely develop in direct contact with the host cell cytoplasm, proliferative stages and spores being often enclosed in vesicles of different origin. They are characterized by polysporoblastic sporogony (in case of dimorphic species at least one of sporogonies is polysporoblastic).

Interestingly, in the extended state, the polar tube of *G. paramecii* is about three times longer, than when it is semi-coiled inside the spore, probably, suggesting telescopic ejection mechanism. Infection with microsporidia in ciliates occurs by means of phagocytosis: the spore is first engulfed by the ciliate in the course of phagosome formation and then the sporoplasm is ejected by the polar tube upon acidification of the phagosome. The long polar tube is required to deliver the sporoplasm to the epithelial cell from the gut lumen, the diameter of which is enormous compared to the much smaller diameter of the ciliate phagosome. Thus, very likely, there is no need in possessing a long polar tube in microsporidia infecting ciliates. Moreover, occurrence of a very long polar tube could make infection of a ciliate impossible, as in a unicellular host organism, a spore with a long ejected polar tube would face the risk of piercing the target cell through and injecting the sporoplasm outside the host, while in a multicellular

organism there is always a chance of delivering it into one of the host cells. The length of the polar tube may be one of the main constraints, which could explain the low rate of microsporidian infections in ciliates. Noteworthy, most species from Clade IV, subclade B, parasitize the intestine (at least as the primary site of infection), with two remarkable exceptions – developing in the fat body *H. lacustris* and *M. macrocyclopis* – the species, which are closely related to *G. paramecii*. Thus, the short polar tube could be a precondition for transferring from a multicellular host to a unicellular one.

G. paramecii has a single nucleus except for late stages of binary fission and polysporoblastic sporogony, which distinguishes it from *E. binucleata* and *M. macrocyclopis*, both characterized by diplokaryotic spores. Unlike *E. binucleata*, meronts were detected in the originally infected *Paramecium* strain SpM5-3, evidencing for the constant autoinvasion of the host under laboratory conditions.

G. paramecii seems to develop inside a parasitophorous vacuole. The members of the Clade IV, subclade B, rarely develop in the direct contact with the host cell cytosol, quite often the proliferative stages and spores are enclosed in vesicles (sometimes individual ones) of different origin. In many species these vesicles are originated from flattened cisternae of rough ER of the host cell like in *Endoreticulatus* spp. and *Vittaforma corneae* (Cali and Garhy, 1991; Silveira and Canning, 1995; Wang *et al.*, 2005). In several cases, the origin of vesicles has not been resolved as for *Cystosporogenes* spp. (see Supplementary Table S1); besides, a combination of both options is also possible. In case of *H. lacustris*, *Glugoides intestinalis* and *Anostracospora rigaudi* development of a complex envelope including both, the membranes of a sporophorous vesicle and rough ER of the host cell, has been supposed (Larsson *et al.*, 1996; Tokarev *et al.*, 2012; Rode *et al.*, 2013). As for *G. paramecii*, In TEM images, membranes surrounding presporal stages in the host cytoplasm were not very distinct, except, probably, the one enclosing the sporogonal plasmodium, which, as well as groups of sporoblasts, was always enclosed in vesicles in living cell observations (Fig. 1 C, F-G, I-J). The nature of some of these vesicles was obvious, for example, the membranes of the macronuclear envelope (Fig. 1 K), while some might be derived from the ER, like in several other relatives – *H. lacustris*, *Endoreticulatus schubergi* and *E. bombycis* (Cali and Garhy, 1991; Wang *et al.*, 2005; Tokarev *et al.*, 2012; see Supplementary Table S1). Since crystals in ciliates are always enclosed in vesicles, our observations of mature spores inside such vesicles together with the host crystals also argues in favour of the presence of a parasitophorous vacuole, a structure derived from the host membranes. Importantly, the spore is mature. If the parasite occurs under the same membrane as the crystal at the stage of sporoplasm, it would certainly undergo several divisions. In this case, there would be several spores under one membrane with a crystal, which is not the

case. This suggests that the parasite is able to get under the membrane of the host at the late stages of the life cycle when the division no longer occurs, possibly, by fusion of vesicles or by detaching from the ER cisterns together with the crystal primordium. As the perinuclear space is continuous with ER, and assuming that crystal-containing vesicles in ciliates detach from cisternae of ER at least some part of microsporidian population resides in ER or its derivates. However, one could speculate that the presence or absence of the membrane surrounding proliferative stages depends on which cell compartment the sporoplasm happens to be delivered to. Seemingly, the development of the presporal stages may take place wherever the sporoplasm is injected.

Blister-like structures conspicuous in some sporoblasts in TEM images suggest the formation of a sporophorous vesicle (pansporoblast), at least around some of the spores, which is in good agreement with our observations of spores enclosed in individual vesicles made both with DIC and TEM (Fig. 4. C, Fig. 5 D, E). Single-cell vesicles are characteristic of a small number of genera, *Tuzetia, Janacekia, Alfvenia, Nelliemelba* and *Lanatospora* and can be seen only with TEM (Vávra and Larsson, 2014). This list also includes *Euplotespora*, which has individual sporophorous vesicle closely encircling the spore surface. In Fig. 5 D and E we observed the structures similar to those seen in the Fig. 19 in Fokin *et al*. (2008). However, it should be stressed that some spores seem to reside directly in the host cytoplasm, suggesting variability in the life cycle of *G. paramecii*. Interestingly, we once happened to find in the culture medium a spore of *G. paramecii* enclosed in an "envelope" (not shown), which reminded the spores of *C. platyophryae* extruding from *P. terricola*, as observed by Foissner and Foissner (1995). The horseshoe-like structures surrounding some of the spores in the host cytoplasm (Fig. 6 B) resemble phagophore formation in *Dictyostelium discoideum* at the onset of autophagocytosis (Calvo-Garrido *et al.,* 2010). Possibly, *G. paramecii* is able to induce autophagy in its host to egress from the host cell, a well-known the strategy for a number of intracellular pathogens (Friedrich *et al.*, 2012; Gerstenmaier *et al.,* 2015; Miller and Celli, 2016; Szokoli *et al.*, 2016). Alternatively, autophagolysosome formation might trigger autoinfection.

The presence of host membranes surrounding the parasite life stages may highlight some details of its life-history strategies. Although microsporidia are characterized by lytic egress from the host cell, non-lytic egress has been registered in *Nematocida parisii* infecting *Caenorhabditis elegans* (Szumowski *et al.,* 2014). This pathogen exploits host vesicle trafficking system and escapes into the host gut lumen via exocytosis. It should be mentioned that this host has a constant cell number, among them 20 nonrenewable intestine cells. Thus, the loss of each cell would affect host fitness. So, according to the concept of optimal virulence, the parasite tends to egress from the host cell causing minimal harm. Since the ciliate is a unicellular organism, host

cell death would mean the death of the whole organism which is not beneficial for the parasite. Apparently, *G. paramecii* uses a similar strategy of egress to spare the host and disseminates gradually the infectious stages. In support of this suggestion is the presence of all life cycle stages in each host cell throughout all period of cultivation. On the contrary, spores of *Nucleophaga amoebae* (Rozellomycota) infecting amoeba mature and egress simultaneously after cell rupture (Gordetskaya *et al.,* 2019).

The presence of two types of spores, i.e. large and small, revealed in *G. paramecii* argues for a complicated dimorphic life cycle. The occurrence of two size classes of spores with similar morphology is a rare case in Microsporidia. This phenomenon has been previously described in two species - *Vavraia anostraca* from *Artemia* sp. (Crustacea: Anostraca) (Martinez *et al.*, 1992) and *Octotetraspora paradoxa* from *Wilhelmia mediterranea* (Diptera: Simuliidae) (Issi *et al.*, 1990). Although we have observed nearly all stages of the life cycle, our data are insufficient to explain the appearance of the small spores and their destiny. One could hypothesize that the large spores are necessary for egress from the host and dissemination, while the small spores could be used for autoinvasion. Besides, the small spores might be a result of meiosis and theoretically could be considered meiospores. However, neither evidence of karyogamy nor synaptonemal complexes were observed.

Large spores of *G. paramecii* occur in the culture medium, which implies that they are released from the host cell. Theoretically, *G. paramecii* could use several different ways of egress from the host cell – by exocytosis via the cytoproct, by compensatory exocytosis at the sites used for exocytosis of trichocyst, with the burst of hyperinfected *Paramecium* cell. It is very likely that the spores inside the vesicle are destined for exocytosis from the host cell. Multiple observations of single spores enclosed in a vesicle containing guanine/hypoxanthine crystal suggest that the parasite may hijack the host vesicular traffic (Fig. 1 M). However, so far we have not managed to observe the release of *Globosporidium* spores from infected *P. primaurelia* with any of the techniques used, DIC or TEM. Thus, at present, it is not possible to determine, which of these egress modalities is used. Anyway, a closer examination of the cell cycle is necessary to elucidate this issue.

About 70 microorganisms, including eukaryotes, have been found to infect various *Paramecium* species (Görtz and Fokin, 2009; Kodama and Fujishima, 2009). The *P. aurelia* complex comprises 15 sibling species (Sonneborn, 1974; Aufderheide *et al.*, 1983; Catania *et al.*, 2009), among which are those that are frequently infected with bacteria (e. g., *P. primaurelia, P. biaurelia, P. tetraurelia, P. pentaurelia, P. sexaurelia, P. octaurelia*) and those that are seemingly not susceptible to any infection (e.g., *P. septaurelia,, P. undecaurelia, P. dodecaurelia*) (Fokin, 2004; Görtz and Fokin, 2009; Schweikert *et al.*, 2013). Not a single

representative of the *P. aurelia* species complex has ever been registered to host a eukaryote, either mutualistic or parasitic. In our study the outcome of the experimental infection for various *Paramecium* species was different. *G. paramecii* demonstrated strong host specificity for only two species, *P. primaurelia* and *P. pentaurelia*, of several tested (see Table 1), which could be explained by close phylogenetic relationships of these two sibling species (Catania *et al.*, 2009). Infection of the *P. caudatum* VL18-5 strain should be considered non-specific, since the strain died out in less than 3 days as a result of hyperinfection, implying the absence of the host control of infection.

G. paramecii, like *E. binucleata*, the microsporidium from the other ciliate, *Euplotes woodruffi*, which underwent molecular characterization, does not group with basal Microsporidia, suggesting that microsporidian infection in ciliates is a recent acquisition. Molecular and phylogenetic data demonstrated, as it would be expected, that these two species are closely related, since both parasitize the cytoplasm of ciliated organisms. Comparing *G. paramecii* with *E. binucleata*, the most accurate morphological differences are dimorphism versus monomorphism, as well as monokaryotic versus diplokaryotic development. Presumably, microsporidian infection in ciliates is secondary, their ancestors parasitizing other aquatic hosts, crustaceans or insect larvae. To resolve the origin of microsporidiosis in ciliates, a further study involving more data on biodiversity and biology of representatives of this subclade and molecular analysis encompassing a vast range of environmental sequences is indispensable.

Taxonomic summary

Phylum: Microsporidia Balbiani, 1882

Clade 4 *sensu* Vossbrinck *et al.* (2014), Clade IV, subclade B *sensu* Williams *et al.* (2018)

***Globosporidium*, gen nov.**

Diagnosis. Parasite of *Paramecium*; cytoplasmic localization. All life cycle stages monokaryotic. Merogony by binary fission. Meiosis has not been detected so far. The polar tube isofilar and short, making one incomplete coil. A typical polar sac-anchoring disk complex. The polaroplast is bipartite, with a small vesicular anterior part and a sac-like posterior part. A large posterior vacuole present in the mature spores.

Closely related to the genera *Euplotespora*, *Helmichia* and *Mrazekia*, based on SSU rRNA phylogeny.

Type species: *Globosporidium paramecii* – by monotypy.

Etymology. The genus name refers to the characteristic spherical shape of the spore. Globus (lat.) – a sphere.

***Globosporidium paramecii*, sp. nov.**

Diagnosis. Parasite of *Paramecium primaurelia* and *Paramecium pentaurelia*. The species diagnosis corresponds to that of the genus. Dimorphic, two types of regular spherical spores differing in size. Presporogonial stages, as seen in unfixed squashed host cells, are bound by an envelope of enigmatic origin. Sporonts and sporoblasts in groups of 2, 4 and 6. Sporogony by rosette-like budding. Living large spores 3.7 ± 0.2 µm in diameter, living small spores 1.9 ± 0.2 µm. Spore wall is two-layered with a remarkably thin endospore. Some of the spores enclosed in the host cell membrane.

Type host: *Paramecium primaurelia* (Ciliophora, Alveolata).

Type locality: a pool in Guadalmedina riverbed in Malaga, Spain (36°44'53.6"N, 4°25'28.8"W).

Type material: Thin sections of paraffin-embedded paramecia stained with hematoxylin and eosin, fuchsin and Giemsa stained squashed host cells and Epon embedded ciliates for TEM as well as frozen isolated total DNA of the parasite and its host are stored at the Department of Cytology and Histology, Faculty of Biology, Saint Petersburg University.

Images of living and fixed infected paramecia are kept at the image collection of the same department.

Etymology: The species name alludes to the host genus, *Paramecium*.

Gene sequences: GenBank accession numbers: MN595900.

Acknowledgements

We are thankful to Prof. Irma Issi for fruitful discussion and valuable comments and to Prof. Sergey Karpov for encouragement and support.

Financial support

This work was supported by the Russian Foundation for Basic Research grant 18-04-00562a to ES (light, fluorescent and electron microscopy, experimental infections), Russian Science Foundation grant 19-74-20136 to EN (SSU sequencing and molecular phylogeny) and Russian Science Foundation grant 16-14-10157 to AP (identification of the host species). This study utilized equipment of the Saint Petersburg University Science Park (Resource Centre "Culture Collection of Microorganisms" (RC CCM), Core Facility Centers and "Development of molecular and cell technologies", "Microscopy and Microanalysis").

Conflict of interest

None.

Ethical standards

Not applicable.

References

Aufderheide KJ, Daggett, P-M, Nerad TA (1983) *Paramecium sonneborni* n. sp., a new member of the *Paramecium aurelia* species-complex. *The Journal of Protozoology* **30**, 128-131. doi: 10.1111/j.1550-7408.1983.tb01046.x.

Bass D, Czech L, Williams BA, Berney C, Dunthorn M, Mahé F, Torruella G, Stentiford GD Williams TA (2018) Clarifying the relationships between Microsporidia and Cryptomycota. *Journal of Eukaryotic Microbiology* **65**, 773-782. doi: 10.1111/jeu.12519.

Cali A, El Garhy M (1991) Ultrastructural study of the development of *Pleistophora schubergi* Zwölfer (Protozoa, Microsporidia) in larvae of the spruce budworm, *Choristoneura fumiferane* and its subsequent taxonomic change to the genus *Endoreticulatus*. *The Journal of Protozoology* **38**, 271-278. doi: 10.1111/j.1550-7408.1991.tb04442.x.

Calvo-Garrido J, Carilla-Latorre S, Kubohara Y, Santos-Rodrigo N, Mesquita A, Soldati T, Golstein P, Escalante R. (2010) Autophagy in *Dictyostelium*: genes and pathways, cell death and infection. *Autophagy* **6**, 686-701. doi: 10.4161/auto.6.6.12513.

Castelli M, Serra V, Senra MVX, Basuri CK, Soares CAG, Fokin SI, ModeoL, Petroni G (2019) The hidden world of Rickettsiales symbionts: "Candidatus Spectririckettsia obscura", a novel bacterium found in Brazilian and Indian *Paramecium caudatum*. *Microbial Ecology* **77**, 748-758. doi: 10.1007/s00248-018-1243-8.

Catania F, Wurmser F, Potekhin AA, Przybos E, Lynch M (2009) Genetic diversity in the *Paramecium aurelia* species complex. *Molecular Biology and Evolution* **26**, 421-431. doi: 10.1093/molbev/msn266.

Corsaro D, Walochnik J, Venditti D, Müller K-D, Hauröder B, Michel R (2014a) Rediscovery of *Nucleophaga amoebae*, a novel member of the Rozellomycota. *Parasitology Research* **113**, 4491-4498. doi: 10.1007/s00436-014-4138-8.

Corsaro D, Walochnik J, Venditti D, Steinmann J, Müller K-D, Michel R (2014b) Microsporidia-like parasites of amoebae belong to the early fungal lineage Rozellomycota. *Parasitology Research* **113**, 1909-1918. doi: 10.1007/s00436-014-3838-4.

Corsaro D, Michel R, Walochnik J, Venditti D, Müller K-D, Hauröder B, Wylezich C (2016) Molecular identification of *Nucleophaga terricolae* sp. nov. (Rozellomycota), and new insights on the origin of the Microsporidia. *Parasitology Research* **115**, 3003-3011. doi: 10.1007/s00436-016-5055-9.

Didier ES, Weiss LM. (2006) Microsporidiosis: current status. *Current Opinion in Infectious Diseases*. **19(5)**, 485-492.

Edgar RC (2004) MUSCLE: multiple sequence alignment with high accuracy and high throughput. *Nucleic Acids Research* **32**, 1792-1797. doi: 10.1093/nar/gkh340.

Foissner I, Foissner W (1995) *Ciliatosporidium platyophryae* nov. gen., nov. spec. (Microspora incerta sedis), a parasite of *Platyophrya terricola* (Ciliophora, Colpodea). *European Journal of Protistology* **31**, 248-259. doi: 10.1016/S0932-4739(11)80088-X.

Fokin SI (2004) Bacterial endocytobionts of Ciliophora and their interactions with the host cell. *International Review of Cytology*, 181-249. doi: 10.1016/S0074-7696(04)36005-5.

Fokin SI (2010) *Paramecium* genus: biodiversity, some morphological features and the key to the main morphospecies discrimination. *Protistology* **6**, 227-235.

Fokin SI (2012) Frequency and biodiversity of symbionts in representatives of the main classes of Ciliophora. *European Journal of Protistology* **48**, 138-148. doi: 10.1016/j.ejop.2011.12.001.

Fokin, S.I., Serra, V., Ferrantini, F., Modeo, L., Petroni, G. (2019) "*Candidatus* Hafkinia simulans" gen. nov., sp. nov., a novel Holospora-like bacterium from the macronucleus of the rare brackish water ciliate *Frontonia salmastra* (Oligohymenophorea, Ciliophora): multidisciplinary characterization of the new endosymbiont and its host. *Microbial Ecology* **77**, 1092-1106. doi: 10.1007/s00248-018-1311-0.

Fokin SI, Di Giuseppe G, Erra F, Dini F (2008) *Euplotespora binucleata* n. gen., n. sp. (Protozoa: Microsporidia), a parasite infecting the hypotrichous Ciliate *Euplotes woodruffi*, with observations on microsporidian infections in Ciliophora. *Journal of Eukaryotic Microbiology* **55**, 214-228. doi.org/10.1111/j.1550-7408.2008.00322.x.

Fokin SI, Görtz H-D (2009) Diversity of *Holospora* bacteria in *Paramecium* and their characterization. In Fujishima M (ed). *Endosymbionts in Paramecium*. Springer, Berlin, Heidelberg, 161-199. doi: 10.1007/978-3-540-92677-1_7.

Friedrich N, Hagedorn M, Soldati-Favre D, Soldati T (2012) Prison break: pathogens' strategies to egress from host cells. *Microbiology and Molecular Biology* **76**, 707-720. doi: 10.1128/MMBR.00024-12.

Galindo LJ, Torruella G, Moreira D, Timpano H, Paskerova G, Smirnov A, Nassonova E, López-García P (2018) Evolutionary genomics of *Metchnikovella incurvata* (Metchnikovellidae): an early branching icrosporidium. *Genome Biology and Evolution* **10**, 2736-2748. doi: 10.1093/gbe/evy205.

Gerstenmaier L, Pilla R, Herrmann L, Herrmann H, Prado M, Villafano GJ, Kolonko M, Reimer R, Soldati T, King JS, Hagedorn M (2015) The autophagic machinery ensures nonlytic transmission of mycobacteria. *Proceedings of the National Academy of Sciences* **112(7)**, E687-E692. doi: 10.1073/pnas.1423318112.

Gordetskaya O, Mesentsev Y, Kamyshatskaya O, Michel R, Walochnik J, Smirnov AV, Nassonova ES (2019) Real-time observations on the development of intra- nuclear parasite

Nucleophaga amoebae (Rozellomycota) in the culture of *Thecamoeba quadrilineata*. *Protistology.* 13 (4), 236-245. doi: 10.21685/1680-0826-2019-13-4-6.

Görtz H-D (1987) Infections of *Stentor roesli* and *S. polymorfus* (Ciliophora, Heterotrichisa) by microsporidia. *Parasitology Research* **74**, 34-35.

Görtz H-D (2010) Microbial infections in free-living protozoa. *Critical Reviews in Immunology* **30**, 95-106.

Görtz H-D, Fokin SI (2009) Diversity of endosimbiotic bacteria in *Paramecium*. In Fujishima M (ed). *Endosymbionts in Paramecium*. Springer, Berlin, Heidelberg, pp. 131-160. doi: 10.1007/978-3-540-92677-1_6.

Gouy M, Guindon S, Gascuel O (2009) SeaView Version 4: A multiplatform graphical user interface for sequence alignment and phylogenetic tree building. *Molecular Biology and Evolution* **27**, 221-224. doi: 10.1093/molbev/msp259.

Han B, Weiss LM (2017). Microsporidia: obligate intracellular pathogens within the fungal kingdom. *Microbiology Spectrum* **5(2)**. doi: 10.1128/microbiolspec.FUNK-0018-2016.

Hovasse R (1950) *Spirobutschliella chattoni*, nov. gen., sp., Cilié Astome, parasite en Méditerranée du Serpulien *Potamoceros triqueter* L., et parasité par la Microsporidie *Gurleya nova*, sp. nov, Bulletin de l'Institut océanographique, **962**, 1-10.

Issi I.V., Kadyrova M.K., Pushkar E.N., Khodzhaeva L.F., Krylova S.V. (1990) Microsporidia in blackflies – determination and short description of species of microsporidia of the world fauna. Publishing house "FAN" of the Uzbecks Soviet Socialist Republics, Tashkent, U.S.S.R. 124 (in Russian)

Issi IV, Tokarev YS, Voronin VN, Seliverstova EV, Pavlova OA, Dolgikh VV (2010) Ultrastructure and molecular phylogeny of *Mrazekia macrocyclopis* sp.n. (Microsporidia, Mrazekiidae), a microsporidian parasite of *Macrocyclops albidus* (Jur.) (Crustacea, Copepoda). *Acta Protozoologica* **49**, 75-84.

Karpov S, Mamkaeva M, Aleoshin V, Nassonova E, Lilje O, Gleason F (2014) Morphology, phylogeny, and ecology of the aphelids (Aphelidea, Opisthokonta) and proposal for the new superphylum Opisthosporidia. *Frontiers in Microbiology* **5**, 112. doi: 10.3389/fmicb.2014.00112.

Keeling PJ (2014) Phylogenetic place of Microsporidia in the tree of eukaryotes. In Weiss LM and Becnel JJ (eds.) *Microsporidia: Pathogens of Opportunity*, pp. 19-202. doi: 10.1002/9781118395264.ch5.

Keeling PJ, Fast NM, Corradi N (2014) Microsporidian genome structure and function. In Weiss LM and Becnel JJ (eds.) *Microsporidia: Pathogens of Opportunity*, pp. 221-229. doi: 10.1002/9781118395264.ch7.

Krüger F (1956) Über die Microsporidien-Infektion von *Campanella umbellaria* (Ciliata, Peritricha). *Zoologischer Anzeiger* **156**, 125-129.

Kodama Y, Fujishima M (2010) Secondary symbiosis between *Paramecium* and *Chlorella* Cells. *International Review of Cell and Molecular Biology* **279**, 33-77. doi: 10.1016/S1937-6448(10)79002-X.

Kyei-Poku G, Gauthier D, Schwarz R, Frankenhuyzen K van (2011) Morphology, molecular characteristics and prevalence of a *Cystosporogenes* species (Microsporidia) isolated from *Agrilus anxius* (Coleoptera: Buprestidae). *Journal of Invertebrate Pathology* **107**, 1-10. doi: 10.1016/j.jip.2010.12.010.

Lanzoni O, Fokin SI, Lebedeva N, Migunova A, Petroni G, Potekhin A (2016) Rare freshwater ciliate *Paramecium chlorelligerum* (Kahl, 1935) and its macronuclear symbiotic bacterium "*Candidatus Holospora parva*". *PLOS ONE* **11(12)**, e0167928. doi: 10.1371/journal.pone.0167928.

Lanzoni O, Sabaneyeva E, Modeo L, Castelli M, Lebedeva N, Verni F, Schrallhammer M, Potekhin A, Petroni G (2019) Diversity and environmental distribution of the cosmopolitan endosymbiont "*Candidatus* Megaira". *Scientific Reports* **9(1)**, 1179. doi.org/10.1038/s41598-018-37629-w.

Larsson JIR, Ebert D, Vávra J, Voronin VN (1996) Redescriptjon of *Pleistophora intestinalis* Chatton, 1907, a microsporidian parasite of *Daphnia magna* and *Daphnia puiex*, with establishment of the new genus *Glugoides* (Microspora, Glugeidae). *European Journal of Protistology* **32**, 251-261. doi.org/10.1016/S0932-4739(96)80024-1.

Larsson JIR (2014) The Primitive microsporidia. In Weiss LM and Becnel JJ (eds.) *Microsporidia: Pathogens of Opportunity*, pp. 605-634. doi.org/10.1002/9781118395264.ch24.

Lom J, Nilsen F (2003) Fish microsporidia: fine structural diversity and phylogeny. *International Journal for Parasitology* **33**, 107-127. doi.org/10.1016/S0020-7519(02)00252-7.

Lutz A, Splendor A (1908) Überpebrine und verwandte Microsporidien.Zweite Mitteilung. Centralbl. Bakteriol. Parasitenkd. Infektionskr Hyg Abt 1 Orig **46**, 311-315.

Martinez, M. A., Vivarès, C. P., Rocha, R. D., Fonseca, A. C., Andral, B. and Bouix, G. (1992). Microsporidiosis on *Artemia* (Crustacea, Anostraca): light and electron microscopy of *Vavraia anostraca* sp. nov. (Microsporidia, Pleistophoridae) in the Brazilian solar salterns. *Aquaculture* **107**, 229–237.

Michel R, Schmid, EN, Böker T, Hager DG, Müller K-D, Hoffmann R, Seitz HM (2000) *Vannella sp*. harboring Microsporidia-like organisms isolated from the contact lens and inflamed eye of a female keratitis patient. *Parasitology Research* **86**, 514-520. doi: 10.1007/s004360050704

Michel R, Hauröder B, Zöller L (2009a) Isolation of *Thecamoeba quadrilineata* harboring intranuclear sporeforming endoparasites considered to be fungal organisms. *Acta Protozoologica* **48**, 1-49.

Michel R, Müller KD, Hauröder B (2009b) A novel microsporidian endoparasite replicating within the nucleus of *Saccamoeba limax* isolated from a pond. *Endocytobiosis and Cell Research* **19**, 120-126.

Michel R, Muller K-D, Schmid EN, Theegarten D, Hauroder B, Corsaro D (2012) Isolation of *Thecamoeba terricola* from bark of *Platanus occidentalis* harbouring spore-forming eukaryotic endoparasites with intranuclear development. *Endocytobiosis and Cell Research* **22**, 37-42.

Mikhailov KV, Simdyanov TG, Aleoshin VV, (2017) Genomic survey of a hyperparasitic microsporidian *Amphiamblys sp.* (Metchnikovellidae). *Genome Biology and Evolution* **9**, 454-467. doi: 10.1093/gbe/evw235.

Miller C, Celli J (2016) Avoidance and subversion of eukaryotic homeostatic autophagy mechanisms by bacterial pathogens. *Journal of Molecular Biology* **428**, 3387-3398. doi: 10.1016/j.jmb.2016.07.007.

Miller MA, Pfeiffer W, Schwartz T (2010) Creating the CIPRES Science Gateway for inference of large phylogenetic trees, in: 2010 Gateway Computing Environments Workshop (GCE). Presented at the 2010 Gateway Computing Environments Workshop (GCE), IEEE, New Orleans, LA, USA 1–8. doi: 10.1109/GCE.2010.5676129.

Nowack ECM, Melkonian M (2010) Endosymbiotic associations within protists. Philosophical Transactions of the Royal Society B **365**, 699-712. doi: 10.1098/rstb.2009.0188.

Quandt CA, Beaudet D, Corsaro D, Walochnik J, Michel R, Corradi N, James TY (2017) The genome of an intranuclear parasite, *Paramicrosporidium saccamoebae*, reveals alternative adaptations to obligate intracellular parasitism. *eLife* **6**, e29594. doi.org/10.7554/eLife.29594.

Preer JR, Preer LB (1984) Endosymbionts of protozoa. In Krieg NR (ed) *Bergey's manual of systematic bacteriology*. Williams and Wilkins, Baltimore, pp. 798-811.

Rode NO, Landes J, Lievens EJP, Flaven E, Segard A, Jabbour-Zahab R, Michalakis Y, Agnew P, Vivarès CP, Lenormand T (2013) Cytological, molecular and life cycle characterization of *Anostracospora rigaudi* n. g., n. sp. and *Enterocytospora artemiae* n. g., n. sp., two new microsporidian parasites infecting gut tissues of the brine shrimp *Artemia*. *Parasitology* **140**, 1168-1185. doi: 10.1017/S0031182013000668.

Ronquist F, Teslenko M, van der Mark P, Ayres DL, Darling A, Höhna S, Larget B, Liu L, Suchard MA, Huelsenbeck JP (2012) MrBayes 3.2: Efficient Bayesian phylogenetic inference

and model choice across a large model space. *Systematic Biology* **61**, 539-542. doi: 10.1093/sysbio/sys029.

Schindelin J, Arganda-Carreras I, Frise E, Kaynig V, Longair M, Pietzsch T, Preibisch S, Rueden C, Saalfeld S, Schmid B, Tinevez J-Y, White DJ, Hartenstein V, Eliceiri K, Tomancak P, Cardona A (2012) Fiji: an open-source platform for biological-image analysis. *Nature Methods* **9**, 676. doi: 10.1038/nmeth.2019.

Schweikert M, Fujishima M, Görtz H-D (2013) Symbiotic associations between ciliates and prokaryotes. In Rosenberg E, DeLong EF, Lory S, Stackebrandt E, Thompson F (eds.). *The Prokaryotes* 427-463. doi: 10.1007/978-3-642-30194-0_18.

Silveira H, Canning EU (1995) *Vittaforma corneae* N. Comb. for the human microsporidium *Nosema corneum* Shadduck, Meccoli, Davis & Font, 1990, based on its ultrastructure in the liver of experimentally infected athymic mice. *Journal of Eukaryotic Microbiology* **42**, 158-165. doi: 10.1111/j.1550-7408.1995.tb01557.x.

Skovorodkin IN (1990) A device for immobilizing small biological objects under light optical study. *Tsitologiia* **32**, 301–302.

Sokolova YY, Paskerova GG, Rotari YM, Nassonova ES, Smirnov AV (2014) Description of *Metchnikovella spiralis* sp. n. (Microsporidia: Metchnikovellidae), with notes on the ultrastructure of metchnikovellids. *Parasitology* **141**, 1108-1122. doi: 10.1017/S0031182014000420.

Sokolova YY, Paskerova GG, Rotari YM, Nassonova ES, Smirnov AV (2013) Fine structure of *Metchnikovella incurvata* Caullery and Mesnil 1914 (Microsporidia), a hyperparasite of gregarines *Polyrhabdina sp.* from the polychaete *Pygospio elegans*. *Parasitology* **140**, 855-867. doi: 10.1017/S0031182013000036.

Sonneborn TM (1974) *Paramecium aurelia*. In King RC (ed.). *Handbook of genetics* **2**, 469-594.

Stamatakis A (2014) RAxML version 8: a tool for phylogenetic analysis and post-analysis of large phylogenies. *Bioinformatics* **30**, 1312-1313. doi: 10.1093/bioinformatics/btu033.

Stentiford GD, Becnel JJ, Weiss LM, Keeling PJ, Didier ES, Williams BAP, Bjornson S, Kent ML, Freeman MA, Brown MJF, Troemel ER, Roesel K, Sokolova Y, Snowden KF, Solter L (2016) Microsporidia – emergent pathogens in the global food chain. *Trends in Parasitology* **32**, 336-348. doi: 10.1016/j.pt.2015.12.004.

Stentiford GD, Dunn AM (2014) Microsporidia in aquatic invertebrates. In Weiss LM and Becnel JJ (eds.) *Microsporidia: Pathogens of Opportunity*, pp. 579-604. doi: 10.1002/9781118395264.ch23.

Stentiford GD, Ramilo A, Abollo E, Kerr R, Bateman KS, Feist SW, Bass D, Villalba A (2017) *Hyperspora aquatica* n.gn., n.sp. (Microsporidia), hyperparasitic in *Marteilia cochillia*

(Paramyxida), is closely related to crustacean-infecting microspordian taxa. *Parasitology* **144**, 186-199. doi: 10.1017/S0031182016001633.

Strüder-Kypke MC, Lynn DH (2010) Comparative analysis of the mitochondrial cytochrome *c* oxidase subunit I (COI) gene in ciliates (Alveolata, Ciliophora) and evaluation of its suitability as a biodiversity marker. *Systematics and Biodiversity* **8**, 131-148. doi: 10.1080/14772000903507744.

Szokoli F, Sabaneyeva E, Castelli M, Krenek S, Schrallhammer M, Soares CAG, da Silva-Neto ID, Berendonk TU, Petroni G (2016) "*Candidatus Fokinia solitaria*", a novel "stand-alone" symbiotic lineage of Midichloriaceae (Rickettsiales). *PLoS ONE* **11**, e0145743. doi: 10.1371/journal.pone.0145743.

Szumowski SC, Botts MR, Popovich JJ, Smelkinson MG, Troemel ER (2014) The small GTPase RAB-11 directs polarized exocytosis of the intracellular pathogen *N. parisii* for fecal-oral transmission from *C. elegans.Proceedings of the National Academy of Sciences* 111 (**22**), 8215-8220. doi: 10.1073/pnas.1400696111

Tokarev YS, Voronin VN, Seliverstova EV, Grushetskaya TA, Issi IV (2012) Ultrastructure and molecular phylogenetics of *Helmichia lacustris*, a microsporidium with an uncoiled isofilar polar filament. *Parasitology Research* **110**, 1201-1208. doi: 10.1007/s00436-011-2614-y.

Vávra J (1959) Beitrag zur Cytologie einiger Mikrosporidien. *Věstník Československé zoologické společnosti* **23(4)**, 347-350.

Vávra J (1972) Detection of polysaccharides in microsporidian spores by means of the periodic acid-thiosemicarbazide-silver proteinate test. *Journal of Microscopy* **14**, 357–360.

Vávra J, Larsson JIR (2014) Structure of Microsporidia. In Weiss LM and Becnel JJ (eds.) *Microsporidia: Pathogens of Opportunity*, pp. 1-70 doi:10.1002/9781118395264.ch1

Vávra J, Lukeš J (2013) Microsporidia and 'The Art of Living Together'. *Advances in Parasitology* **82**, 253-319. doi.org/10.1016/B978-0-12-407706-5.00004-6.

Vossbrinck CR, Debrunner-Vossbrinck BA, Weiss LM (2014) Phylogeny of the Microsporidia. In Weiss LM and Becnel JJ (eds.) *Microsporidia: Pathogens of Opportunity*, pp. 203-220. doi: 10.1002/9781118395264.ch6.

Vossbrinck RC, Debrunner-Vossbrinck AB (2005) Molecular phylogeny of the Microsporidia: ecological, ultrastructural and taxonomic considerations. *Folia Parasitologica* **52**, 131-142.

Wang C-Y, Solter LF, T'sui W-H, Wang C-H (2005) An *Endoreticulatus* species from *Ocinara lida* (Lepidoptera: Bombycidae) in Taiwan. *Journal of Invertebrate Pathology* **89**, 123–135. doi: 10.1016/j.jip.2005.03.002.

Weiss LM, Vossbrinck CR (1999) Molecular biology, molecular phylogeny, and molecular diagnostic approaches to the Microsporidia. In Wittner M and Weiss LM (eds) *The Microsporidia and Microsporidiosis,* pp. 129-171.

Williams BAP, Hamilton KM, Jones MD, Bass D (2018) Group-specific environmental sequencing reveals high levels of ecological heterogeneity across the microsporidian radiation: Ecological heterogeneity in the microsporidia. *Environmental Microbiology* **10**, 328-336. doi: 10.1111/1758-2229.12642.

Zhu X, Wittner M, Tanowitz HB, Kotler D, Cali A, Weiss LM (1993) Small subunit rRNA sequence of *Enterocytozoon bieneusi* and its potential diagnostic role with use of the polymerase chain reaction. *The Journal of Infectious Diseases* **168**, 1570-1575. doi: 10.1093/infdis/168.6.1570.

Table 1. The list of the tested endobiont-free *Paramecium* cultures and the results of the experimental infections.

Strain	Species	Year of isolation	Place of isolation	Presence of infection by			GenBank Accession number	COI sequence identity (%)
				3rd day	7th day	14th day		
IP1-2	*P. biaurelia*	2015	Italy, Pisa	-	-	-	KX008305	99.8
UB-15	*P. novaurelia*	2014	Russia, Leningrad district	-	-	-	MG013511	98.4
IP3-20	*P. primaurelia*	2015	Italy, Pisa	+	+	+	MG589324	100
Sp9-33	*P. triaurelia*	2014	Spain, Madrid	-	-	-	JX010633	99.8
ETu 7-11	*P. biaurelia*	2016	Estonia, Tartu	-	-	-	KX008305	100
NR-2	*P. pentaurelia*	2016	USA, NE, Niobrara river	+	+	+	MG589325	100
CyL8-8	*P. primaurelia*	2014	Cyprus, Larnaca, city	+	+/NA	+/NA	MH188082	100
CyL10-4	*P. sonneborni*	2012	Cyprus, Larnaca, Oroklini	-	-	-	KF650001	99.5
87	*P. pentaurelia*	1974	USA, Sonneborn Collection	+	+	+/-	EU086118	100
Nr1-9	*P. pentaurelia*	2016	Russia, Novorossiysk	+	+	+/NA	MG589325	100
VL18-5	*P. caudatum*	2016	Russia, Vladimir	+	NA	NA		
BMK15	*P. caudatum*	2015	Russia, the White Sea	-	-	-		

+/NA In one replicate all infected cells of the strain died by the day specified in table
+/- Not all of the tested cells were infected by the 14th day
NA Data are not available, because the cells died by the day specified in the table

Legends for figures

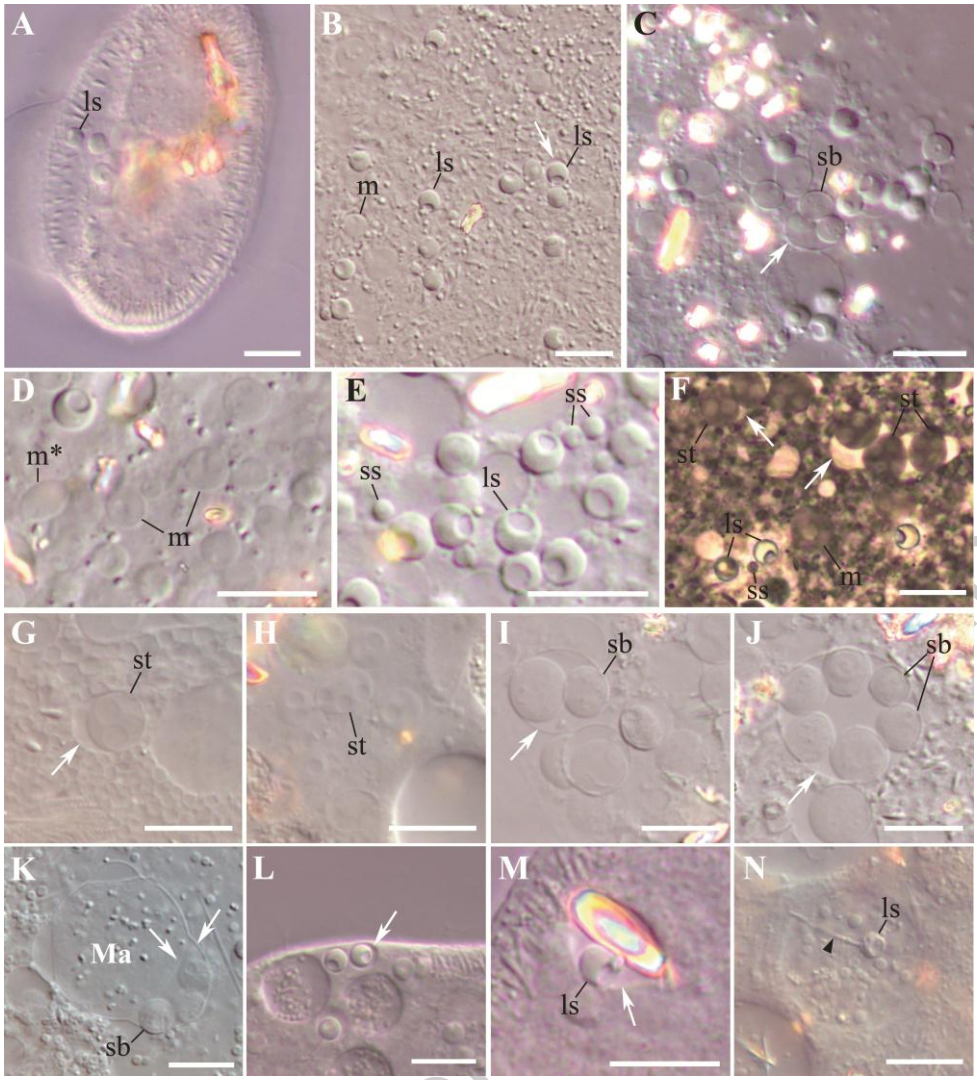

Figure 1. Living microsporidia *Globosporidium paramecii* parasitizing in the cytoplasm of *Paramecium* spp. **A-C**. Isolated from nature originally infected *P. primaurelia* SpM5-3. **D-N**. Experimental infections. **D-H**, **I-M.** *P. primaurelia* IP3-20. **G**, **H**. *P. pentaurelia* NR-2. **N**. *P. caudatum* VL18-5. **A.** A living paramecium with three spores in the focal plane. **B.** Conspicuous spherical spores (one in a vesicle labeled with a white arrow) and meronts from the cytoplasm of the squashed host cell. **C.** Sporoblasts in a vesicle. **D.** Meronts; note the meront dividing by binary fission. **E.** Two types of spherical spores, large and small. **F-H**. Diversity of life cycle stages: meront appears to be in direct contact with the host cell cytoplasm, binuclear and tetranuclear sporonts in a common vesicle (**F**), large spores. **I, J.** Groups of two (**I**) and six sporoblasts (**J**) in a vesicle. **K**. Maturing sporoblasts in the perinuclear space of the host macronucleus. Ma – macronucleus. **L**. A large spore enclosed in a host cell membrane, presumably, parasitophorous vacuole. **M.** A large spore enclosed in a host cell membrane together with a crystal. **N.** A large spore with ejected polar tube (black arrowhead) in the phagosome. **A-E** and **G-N** – differential interference contrast, (DIC). **F** – phase contrast. In all

images: large spore (ls), small spore (ss), meront (m), dividing meront (m*), sporont (st), sporoblast (sb), vesicle (white arrrow). Scale bar: 10 µm.

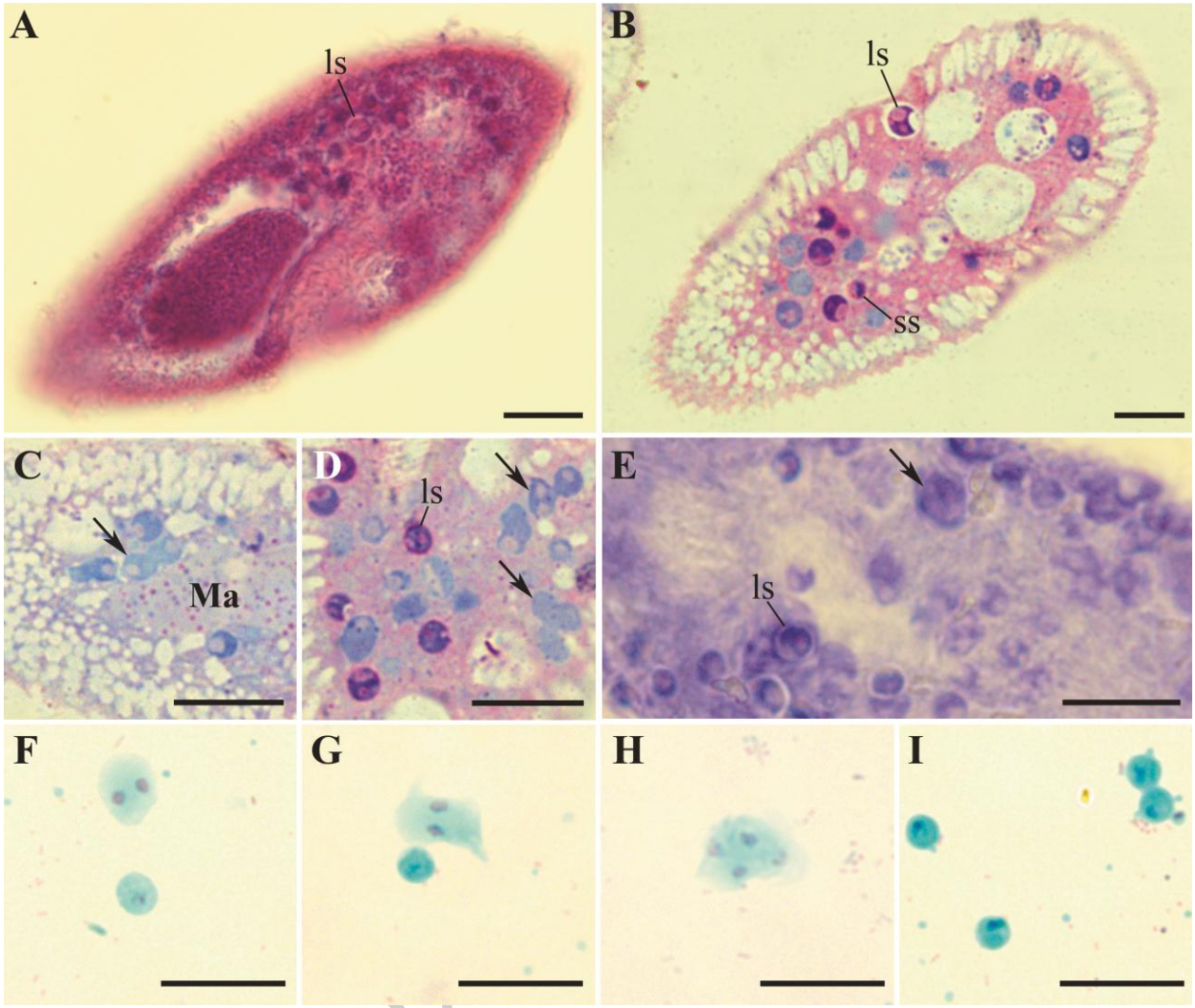

Figure 2. Life cycle stages of *Globosporidium paramecii* from the cytoplasm of *Paramecium primaurelia* revealed with various staining techniques. **A.** A thin section of paraffin-embedded paramecium with numerous spores. Hematoxylin and eosin staining. **B-D.** Life cycle stages of the parasite in semithin sections of initially infected strain SpM5-3, methylene blue and basic fuchsin staining. **E.** Giemsa staining of the squashed and methanol fixed infected paramecium. **F-I.** Nuclear staining in squashed and methanol fixed host cell, stained with fuchsin, counterstained with light green: binuclear proliferative stages (**F**, **G**), tetranuclear sporont (**H**), large spores (**I**). In all images: large spore (ls), small spores (ss), proliferative stages (arrows). Scale bar: 10 µm.

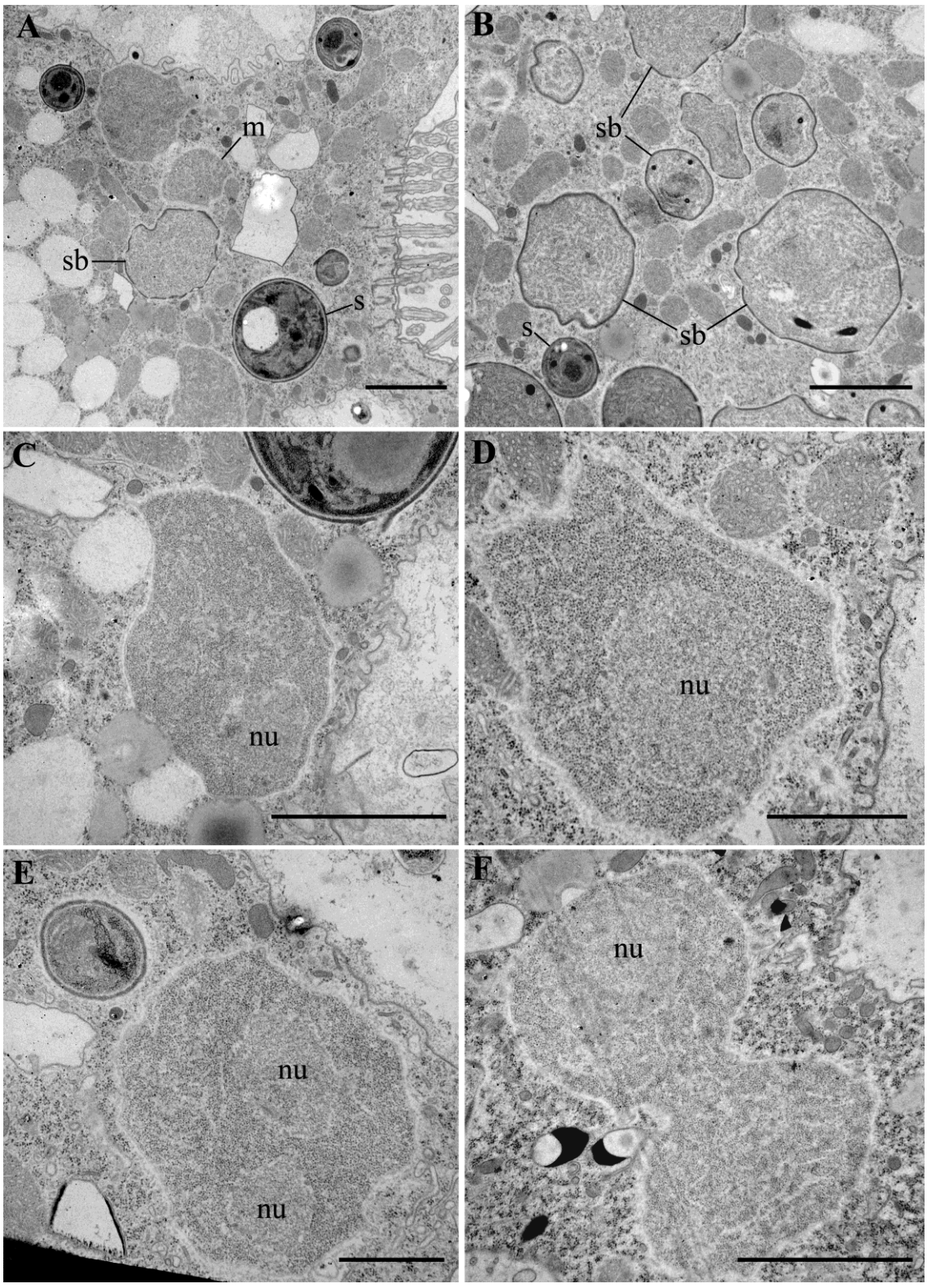

Figure 3. Transmission electron micrographs (TEM) of the originally infected *P. primaurelia* strain SpM5-3. **A, B.** A fragment of the infected host cell with meronts (m), sporoblasts (sb) and spores (s) in the cytoplasm. **C, D.** Unikaryotic meront, note host mitochondria adjacent to the parasite. **E, F.** Meront dividing by binary fission. nu – nucleus. Scale bar: A, B, C, F, 2 μm; D, E, 1 μm.

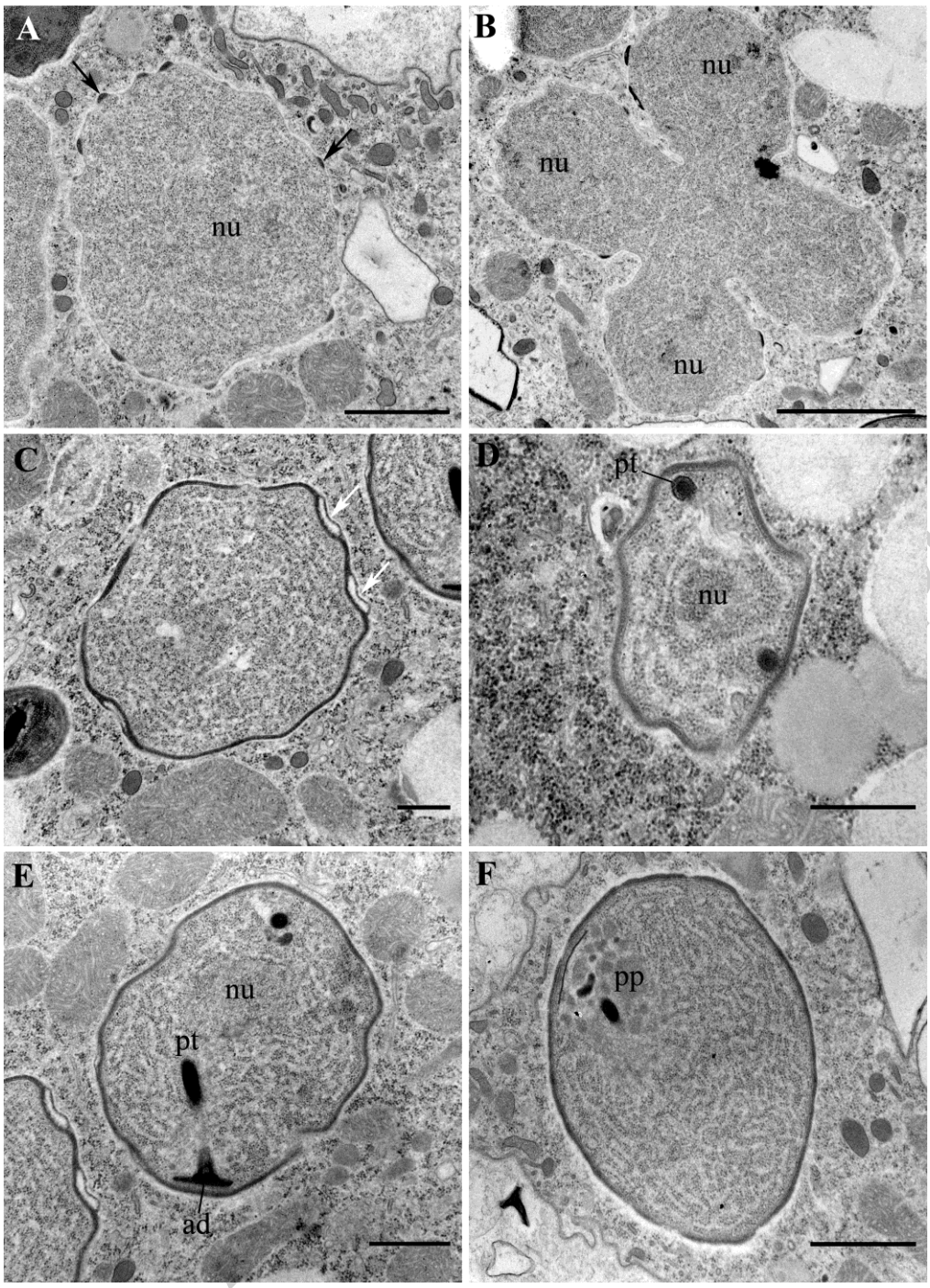

Figure 4. Transmission electron micrographs (TEM) of sporogonial stages of *Globosporidium paramecii* in the originally infected *P. primaurelia* strain SpM5-3. **A.** Transitional stage between meront and sporont, note electron-dense patches of the exospore primordium on the surface of plasma membrane (arrows). **B.** Sporogonial tetranuclear plasmodium. **C.** Early sporoblast with a well-developed exospore forming blister-like structures (white arrows). **D.** Sporoblast with a cross sectioned polar tube (pt). **E.** Late sporoblast with a developed anchoring disk (ad) and a polar tube (pt). **F.** Late sporoblast with a forming polaroplast (pp). nu – nucleus. Scale bar: A, F, 1 μm; B, 2 μm; C, D, E, 500 nm.

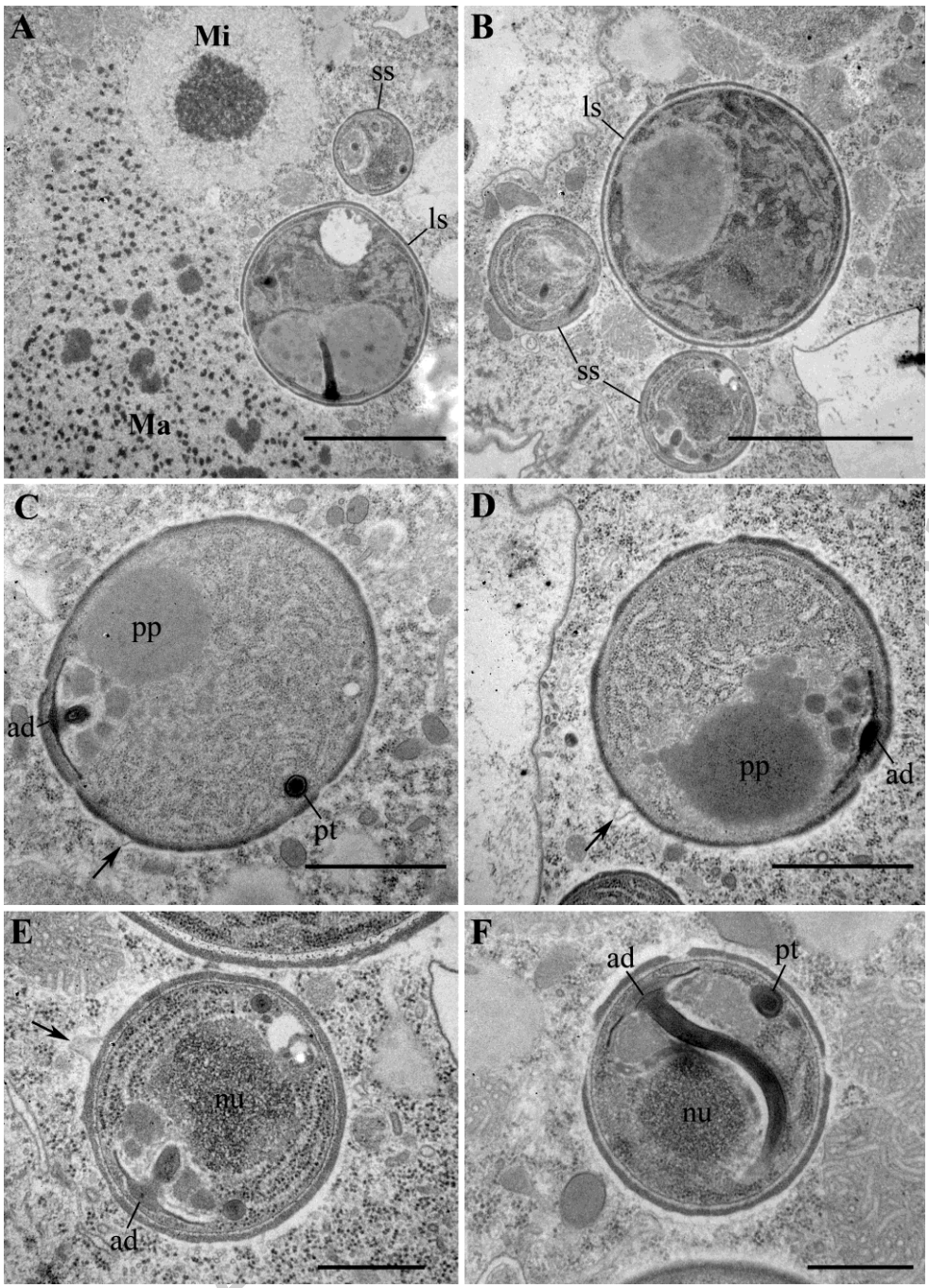

Figure 5. Transmission electron micrographs (TEM) of spores. **A, B**. Two types of spores, large and small, co-occurring in the host cytoplasm. Large spore (ls), small spore (ss), macronucleus (Ma), micronucleus (Mi). **C, D.** Large spores with a polaroplast (pp) and an anchoring disk (ad). Note protrusions of the outer layer of exospore into host cytoplasm (arrows). **E, F**. Small spores with a developed anchoring disk (ad) and an isofilar polar tube (pt). **E,** enlarged fragment of **B.** Scale bar: A, B, E, F, 1 μm; C, D, 500 nm.

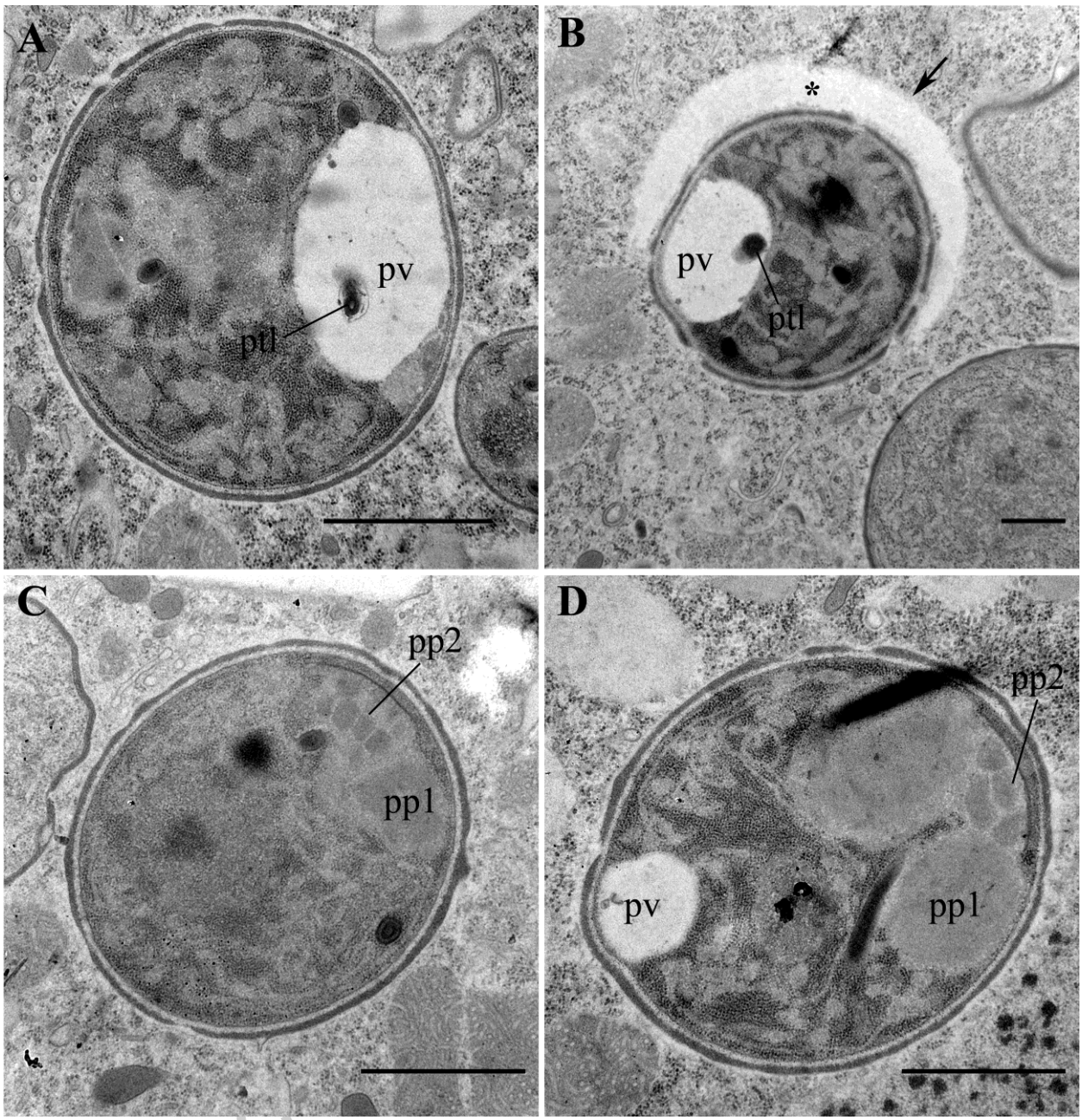

Figure 6. Transmission electron micrographs (TEM) of mature spores. **A.** A large spore with a well-developed posterior vacuole (pv). **B.** A small spore surrounded by a vast horseshoe-like cisterna (asterisk) of the host cell. Note a polar tube-like structure (ptl) inside the posterior vacuole in **A** and **B. C, D.** Large spores with prominent bipartite polaroplast (pp1 and pp2). Scale bar: A, C, D, 1 μm; B, 500 nm.

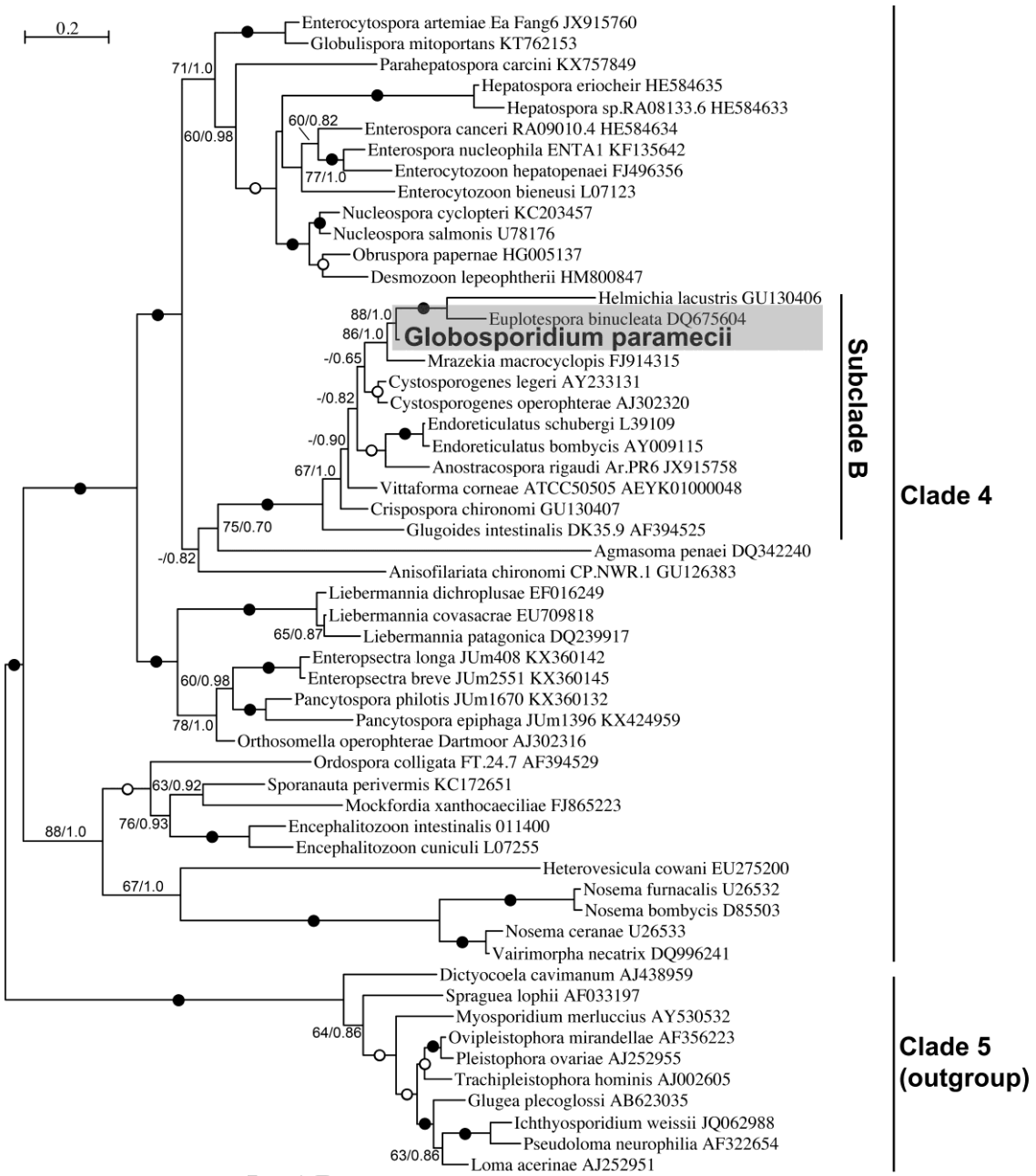

Figure 7. Phylogenetic position of the *Globosporidium paramecii* on a microsporidian tree. Phylogenetic reconstruction based on RAxML and MrBayes analyses of SSU rRNA gene demonstrates the affiliation of microsporidia from ciliates with the representatives of subclade B, Clade 4. Black blobs correspond to the bootstrap support 100% and posterior probability 1.0, the circles correspond to bootstrap support > 95% and posterior probability 1.00. Gray box encloses the microsporidia from the ciliates.